Microfluidic Platform Integrated with Graphene-Gold Nano-composite Aptasensor for One-step Detection of Norovirus

Rohit Chand, Suresh Neethirajan

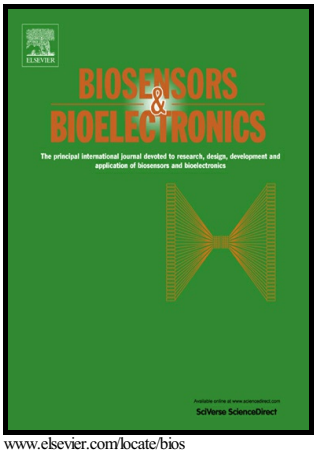

www.elsevier.com/locate/bios

PII: S0956-5663(17)30401-3
DOI: http://dx.doi.org/10.1016/j.bios.2017.06.026
Reference: BIOS9796

To appear in: *Biosensors and Bioelectronic*

Received date: 7 May 2017
Revised date: 13 June 2017
Accepted date: 14 June 2017

Cite this article as: Rohit Chand and Suresh Neethirajan, Microfluidic Platforn Integrated with Graphene-Gold Nano-composite Aptasensor for One-ste Detection of Norovirus, *Biosensors and Bioelectronic* http://dx.doi.org/10.1016/j.bios.2017.06.026

Microfluidic Platform Integrated with Graphene-Gold Nano-composite Aptasensor for One-step Detection of Norovirus

Rohit Chand, Suresh Neethirajan*

BioNano Laboratory, School of Engineering, University of Guelph, Guelph, ON, N1G 2W1, Canada

*Corresponding author: sneethir@uoguelph.ca (S. Neethirajan)

Abstract

Noroviruses are a foremost cause of gastroenteritis outbreaks throughout the world. On-site sample processing and detection of the viral clinical samples has always been a problem. This study reports an all-polydimethylsiloxane microfluidic chip integrated with screen-printed carbon electrode for the electrochemical detection of norovirus. The microfluidic chip contained packed silica microbeads zones to filter and enrich the norovirus infected clinical sample. Selective detection of norovirus was accomplished by functionalizing the graphene-gold nanoparticles composite modified carbon electrode with the viral capsid-specific aptamer. Norovirus specific aptamer was tagged with a ferrocene molecule, which acts a redox probe. The interaction of aptamer and norovirus resulted in a decrease in the electrochemical signal from ferrocene. The microfluidic chip and functionalized electrodes were characterized using several microscopic and electrochemical techniques. The optimized microfluidic aptasensor was employed to detect a range of norovirus concentration. Using differential pulse voltammetric analysis, a detection limit of 100 pM with a detection range from 100 pM to 3.5 nM for norovirus was obtained. The application of aptasensor was also assessed by detecting norovirus in spiked blood samples. The aptasensor could easily discriminate between the target norovirus and other interfering molecules. The developed microfluidic aptasensor has the potential to be used for point-of-care one-step detection of norovirus in clinical samples.

Keywords: Aptamer; Biosensor; Electrochemical detection; Microfluidic chip; Norovirus

1. Introduction:

Noroviruses, belonging to the *Calciviridae* family, are a common cause of food poisoning all over the world (Scallan et al., 2011). Norovirus is an RNA virus that spreads via the fecal-oral route. It is extremely contagious and has been associated with more than 90% of reported non-bacterial gastroenteritis outbreaks in the United States (Koo et al., 2010). Noroviruses are categorized genetically into five genogroups (GI - GV), which are further divided into many genetic clusters or genotypes (White 2014). Out of the five genogroups, Norovirus GII mediated infection is predominant in humans (White 2014). Noroviruses have a very low dose of infection (<100 virions), and are unfortunately fairly resistant to heating and common disinfectants (Hutson et al., 2004). The outbreak is generally limited to a close public area, infecting 10-100s of people at a time. A report suggests that patients typically shed 10^5–10^9 norovirus/g feces for a period of 8-60 days (Teunis et al. 2015). Therefore, it is extremely important to rapidly quantify norovirus in clinical and food samples.

Noroviruses are conventionally detected in clinical samples using enzyme-linked immunosorbent assay (ELISA) or polymerase chain reaction (PCR) including real-time PCR and reverse transcriptase PCR (Bruin et al., 2006; Jiang et al., 1992; Kageyama et al., 2003; Vinje et al., 2003). However, ELISA-based analysis lacks specificity and sensitivity in the case of norovirus detection (Wilhelmi et al., 2007). Additionally, ELISA and PCR analysis require a number of expensive table-top equipment, extended analysis time, and skilled human involvement, making them unfit for on-site analyses. The drawbacks of these convention analyses necessitate the need for a real-time, rapid, and point-of-care biosensing methodology for the detection of norovirus.

For the effective detection of viral pathogens, sample purification and enrichment from the complex background often play an important role. A faster sample processing and detection is required for the positive confirmation of viral presence (Halfon et al., 1996). Analysis for gastroenteritis is generally performed on feces or vomit of the patient (Richards et al., 2004). Processing of feces for analysis requires time-consuming centrifugation and filtration to remove unwanted solid particulates and debris for target purification. During sample processing, a lot of human involvement is required, which increases the risk of infection among health professionals (Friesema et al., 2009). Additionally, availability of centrifuge at all remote locations or on-site is not feasible. Recently, Chung et al. reported a microfluidic nucleic acid amplification mediated detection of murine norovirus (Chung et al., 2015). The integrated microchip also stressed the issue of sample preparation from a complex matrix for norovirus detection.

So far, a number of biosensing platforms have been proposed on providing promising alternatives for norovirus detection. Various modern techniques like interferometry, surface plasmon resonance, field effect transistor, and electrochemical for detection of norovirus has been described (Auer et al., 2015; Hwang et al., 2017; Xiang et al., 2016; Yakes et al., 2013). Recently, Hagström et al. reported a lateral-flow assay for the immunosensing of norovirus (Hagström et al., 2015). Likewise, Hong et al. proposed a pre-emptive electrochemical detection of norovirus using concanavalin A based immunosensing (Hong et al., 2015). Electrochemical biosensors have proved to be selective, sensitive, and rapid. Electrochemical biosensors have been employed to detect several bio-analytes, such as enzymes, viruses, metabolic markers, etc. (da Silva et al., 2017). These biosensors are easy to miniaturize, cost-effective, and label-free. Several bio-recognition receptors like antibodies, aptamers, nucleic acids, etc. can be seamlessly immobilized on the electrode surface for selective detection.

Recently, aptamers have attracted considerable attention because of several advantages over antibodies (Song et al., 2012). Aptamers are easy to design and manufacture, are stable, and have unlimited applications. Aptamers are screened through repeated rounds of systematic evolution of ligands by an exponential enrichment (SELEX) process. Discovery of aptamers for norovirus targeting is a part of much research and several such aptamers have been discovered (Beier et al., 2014; Escudero-Abarca et al., 2014). Aptamer-based biosensors (aptasensor) with electrochemical detection have also been commonly employed to detect norovirus (Giamberardino et al., 2013; Hwang et al., 2017; Kitajima et al., 2016). The common principle behind the majority of these biosensors is that the interaction of aptamer and norovirus increases the impedance of the local electrode surface. Due to the increased impedance, a reduced electrochemical signal was obtained in the presence of potassium ferricyanide/ferrocyanide ($[Fe(CN)_6]^{3-/4-}$) redox couple dissolved in the buffer solution. Though these biosensors reported good sensitivities, the use of potassium ferricyanide/ferrocyanide as a redox couple has multiple disadvantages. The addition of redox couple in buffer adds an additional step and is not suitable for multiplexing and point-of-care devices (Fernandes et al., 2014). Additionally, several reports suggest that potassium ferricyanide/ferrocyanide redox couple cannot be used for quantitative measurements in gold based electrodes (Dijksma et al., 2002; Vogt et al., 2016). The release of CN^- ions from $[Fe(CN)_6]^{3-/4-}$ during electrochemistry seriously damages the gold surface and results in desorption of functional molecules. Redox probes, such as potassium ferricyanide and ruthenium complexes, are in general light and moisture sensitive and therefore need to be made fresh before every analysis (Dijksma et al., 2002). This reduces the shelf-life of methodology, if commercially developed.

The sensitivity of the electrochemical detection can be highly enhanced by modifying electrode with nanomaterials, such as gold nanoparticles (AuNPs), magnetic nanoparticles,

nanofibers, graphene, etc. (Lan et al., 2017). Over the past few years, nano-composites have proven to be excellent transducers in electrochemical sensors (Shrivastava et al., 2016). Nano-composites are low cost and easy to synthesize and offer enhanced electronic properties, high surface ratio, controllable electrochemical properties, and biocompatibility. Components of nano-composites retain their distinct properties, as well as impart novel properties resulting from their combination. In particular, several graphenes (Grp) and nanoparticles (NPs) based composites have become a popular substrate in many electrochemical sensors (Veerapandian and Neethirajan 2015; Ahmed et al., 2017). Grp-NPs composite possess the dual advantages of Grp (large surface area, high electrical conductivity, and excellent mechanical strength) and the respective nanoparticle (conductivity, selectivity, a substrate for functionalization, etc.). The Grp-NPs composite can be easily layered on electrodes using drop casting, spin coating, or ink-jet printing to prepare thin conductive film (Veerapandian and Neethirajan 2015). Commercially available screen-printed carbon electrodes (SPCE) have also become a desirable electrochemical sensing platform for cost-effective and promptly practicable disposable devices. However, they have seldom been integrated with microfluidic devices to fabricate a disposable lab-on-a-chip.

Herein, we developed an integrated aptasensor for norovirus detection, considering the importance of sample processing, nano-composites, and redox probe free buffer towards the point-of-care application. This work proposes a proof-of-concept for the electrochemical sensing of norovirus using commercially available aptamer on the disposable microfluidic platform. The microfluidic chip integrates microbeads based microfiltration zone and Grp-AuNPs composite modified the electrochemical sensing zone. Packed silica microbeads were used to filter out solid or larger sized particles from the solution. The Grp-AuNPs composite provided a durable substrate for aptamer immobilization, along with enabling amplified electron transfer process at the interface. A ferrocene tagged aptamer, rather than $[Fe(CN)_6]^{3-}$

$^{/4-}$ mixed buffer, specific to Norovirus GII was used for the detection. The interaction of aptamer and norovirus trapped the ferrocene within the complex, thus increasing the capacitance of the electrode. The reduction in electrochemical signal was used to quantify the norovirus. The developed microfiltration zone and modified electrodes were characterized using optical microscopy, UV-visible spectroscopy, transmission electron microscopy, and electrochemical techniques. Developed biosensing microfluidic chip has the potential for on-site monitoring and direct detection of norovirus in the clinical samples.

2. Experimental

2.1 Materials

Graphene dispersion was purchased from ACS Material (CA, USA). Hydrogen tetrachloroaurate(III) hydrate ($HAuCl_4 \bullet 3H_2O$), sodium citrate, potassium hexacyanoferrate ($K_4[Fe(CN)_6]$), potassium hexacyanoferrite ($K_3[Fe(CN)_6]$), and phosphate buffer saline (PBS) were purchased from Sigma-Aldrich (ON, Canada). All the chemicals were of analytical grade and used as received without further purification. Milli-Q water (18.2 MΩ, DI water) was used throughout the experiments. Silica microbeads (100 µm) were obtained from OPS Diagnostics (NJ, USA). The carbon screen-printed electrodes (SPCE) used in this study were purchased from Dropsens (model C110, Spain). The working (4 mm diameter) and counter electrode were made of carbon, whereas the reference electrode was made of silver.

Norovirus Group II (recombinant virus-like particle, Norovirus Hu/GII/Beijing/06/2005/CHN) was purchased from MyBioSource (CA, USA). Thiolated streptavidin and bovine blood were purchased from Cedarlane Labs (ON, Canada). The 81-bases-long aptamer for Norovirus GII was synthesized by GeneLink (NY, USA) and the sequence was obtained from Aptagen (PA, USA). The aptamer had the following sequence:

AGTATACCGTATTACCTGCAGCCATGTTTTGTAGGTGTAATAGGTCATGTTAGGG

TTTCTGCGATATCTCGGAGATCTTGC (5′-3’)

The 5′ end of the aptamer was modified with biotin and the 3’ end was modified with the ferrocene redox probe (Bt-Apt-Fc). The lyophilized aptamer was re-suspended in TE buffer (10 mM Tris–HCl, 0.1 mM EDTA, pH 8.0) to a stock concentration of 100 µM. The aptamer was then diluted to the required concentration in 1X PBS.

2.2 Preparation of modified electrodes

Functionalization of graphene with gold nanoparticles was based on the reduction of $HAuCl_4$ by sodium citrate. In brief, different concentrations of aqueous graphene (0.5 and 1 mg/mL) were mixed with 1 mM $HAuCl_4$. The resultant suspensions were boiled at 100 °C on a hotplate for 30 min to promote their interaction. Finally, 38.8 mM of sodium citrate was added dropwise in each of the suspensions and the mixtures were kept under stirring for 1 hour. Upon addition of sodium citrate, the color of solutions changed from greyish-black to red-black. The obtained Grp-AuNps composites were centrifuged and washed repeatedly with DI water to eliminate unused reactants. The final nano-composites were stored in dark at 4 °C for further use. The nano-composites were characterized using UV-visible spectroscopy (Cary 100, Agilent Technologies), energy-dispersive X-ray (EDX) spectroscopy, and transmission electron microscope (TEM, FEI Tecnai G2 F20).

The carbon working electrodes were modified by drop casting 5 µL of the Grp-AuNPs composites and allowed to anneal at 120 °C for 1 hour inside a hot air oven. Three layers were casted to ensure uniform coverage of the electrode surface. All of the modified electrodes were thoroughly rinsed with DI water for further experiments. Cyclic voltammetry was used to analyze the property of the nano-composites modified electrodes.

2.3 Electrode functionalization for aptasensor

Gold nanoparticles embedded in Grp-AuNPs composite were functionalized, as illustrated in Fig. 1B, to achieve a bioactive interface layer for aptasensor. At first, 0.5 mg/mL of thiolated streptavidin, prepared in 1X PBS, was added on the modified electrodes and incubated at 4 °C for 4 hours. Afterward, varying concentrations of Bt-Apt-Fc ranging from 0.25-1.5 µM was drop-casted onto the streptavidin functionalized Grp-AuNPs electrode and incubated at room temperature for 30 min. At the end of each functional layer coating, electrodes were gently rinsed with DI water to remove physio-adsorbed molecules. The immobilization of thiolated streptavidin and aptamer was validated using electrochemical analysis. The aptasensors were stored at 4 °C when not in use.

2.4 Microfluidic chip fabrication

The schematic design of a commercial SPCE integrated all-PDMS based low-cost microfluidic chip is shown in Fig. 1(A). The microfluidic chip consisted of two inlets, microbeads based filtration zone, a sensing zone, and an outlet. The microfluidic chips were fabricated using the standard lithography technique. A silicon and SU-8 based master mold was prepared for making polydimethylsiloxane (PDMS) engraved microchannels. Firstly, an SU-8 negative photoresist (MicroChem, MA, USA) was spin-coated on a clean silicon wafer followed by pre-baking. The photoresist film was then exposed to UV light through a photomask bearing the desired microchannel geometry (Fine Line Imaging, CO, USA). After post-baking and developing, a master mold was obtained. Next, a degassed mixture of PDMS pre-polymer and curing agent (10:1 w/w) was poured over the mold and cured at 75 °C for about 4 hours. The PDMS replica was peeled off the master mold after curing and then the inlets were punched.

A second thin layer of PDMS was molded containing the groove for the SPCE. The two PDMS layer were treated with oxygen plasma for 40 s to produce silane-activated surface. The layers were then aligned under an optical microscope and reversibly bonded. Finally, the aptamer functionalized SPCE were integrated with the PDMS microfluidic chip. To achieve this, a thin layer of epoxy glue was carefully smeared around the electrode. The SPCE were then placed in the groove of the second PDMS layer and left for attachment. The integration of electrode and the microfluidic chip was inspired by the previously reported work (Yoon et al., 2014).

2.5 *Fabrication of microfilter*

Silica microbeads (100 µm) based parallel microfilters were incorporated in the microchip for efficient physical filtration of the sample. The branched microchannels before and after filtration zone helped in distribution and mixing of the sample, respectively. The inlets of the microfiltration zones were 200 µm wide, whereas the outlets were 50 µm wide. Silica microbeads suspension was prepared in the 1X PBS. The microbeads suspension was injected into the sample inlet until the microfiltration zones were visibly full. The narrow (50 µm) opening of the microfiltration zone prevented the entering of microbeads in the sensing zone or clogging of the microchannel.

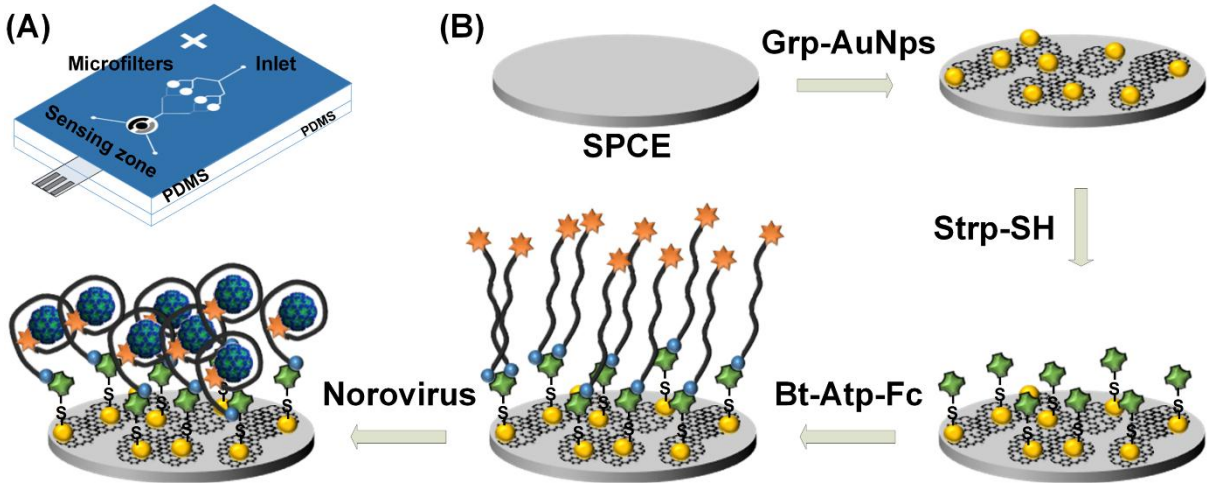

Fig. 1. Microfluidic electrochemical aptasensor for norovirus detection: (A) Structure of PDMS microfluidic chip showing microfilters, sensing zone, and integrated screen-printed carbon electrode (SPCE), (B) Sequence of electrode functionalization and aptasensing of norovirus. Grp-AuNPs: Graphene-gold nanoparticles composite, Strp-SH: Thiolated streptavidin, Bt-Atp-Fc: Biotin and ferrocene tagged aptamer.

2.6 Electrochemical detection of norovirus using aptasensor

The one-step and label-free detection of norovirus was based on aptamer-target interaction. The norovirus capsid protein was captured by the selective Bt-Apt-Fc immobilized on the Grp-AuNPs composite modified electrode. The norovirus sample prepared in 1X PBS was injected into the sensing zone through the microchannel and allowed to interact at room temperature. The interaction time of Bt-Apt-Fc and norovirus was studied from 10-40 min to optimize the analysis. The optimized microfluidic aptasensor was tested for its electrochemical response to varying concentrations of norovirus. The norovirus capsid protein was also spiked to peptidoglycan solution and bovine blood to investigate the selectivity and applicability of the proposed sensor.

All the electrochemical measurements were carried out in triplicates, with the mStat 400 potentiostat from DropSens (Spain). Cyclic voltammetry (CV) and differential pulse voltammetry (DPV) were recorded in 1X PBS. The CV measurements were performed in the potential range from -0.1 to 0.6 V at a scan rate of 100 mV/sec. The DPV measurements were performed in the potential region from 0.1 to 0.6 V at a scan rate of 50 mV/sec with an amplitude of 2 mV and a step potential of 4 mV. A solution 5 mM $K_3[Fe(CN)_6]$ and 5 mM $K_4[Fe(CN)_6]$ in 1X PBS was used for CV, wherever applicable. The SPCE on the integrated microfluidic chip was directly inserted into the electrode holder for electrochemical analysis.

3. Results and discussion

3.1 Characterization of Grp-AuNPs composite and electrode modification

The UV-visible spectroscopic analysis of Grp-AuNPs composites revealed a characteristic plasmonic peak of AuNPs located at 530 nm. No such peak was obtained for pristine Grp (Fig. 2(A)). As shown in Fig. 2(A), UV–visible spectroscopy of pristine Grp and Grp-AuNPs composites exhibited the characteristic π–π* bond of the polyaromatic C–C at 230 nm. The Grp-AuNPs composite with a higher concentration of Grp (1 mg/mL) showed a broader peak of AuNPs, implying a larger size distribution of AuNPs. This is perhaps due to the increased interaction of Grp with $HAuCl_4$, thus hindering the uniform nucleation of AuNPs. The EDX spectroscopy of the Grp-AuNPs composite was performed to verify the components of the nano-composites. The presence of carbon and gold in the elemental composition of Grp-AuNPs composite was also a good indication of the successful synthesis of the desired nano-composite (Fig. S1). The morphology of the Grp-AuNPs composite is shown in Fig. 2(B). The transmission electron microscopic study of Grp-AuNPs composite (Grp=0.5 mg/mL) confirmed the presence of AuNPs with an average size of ~16 nm.

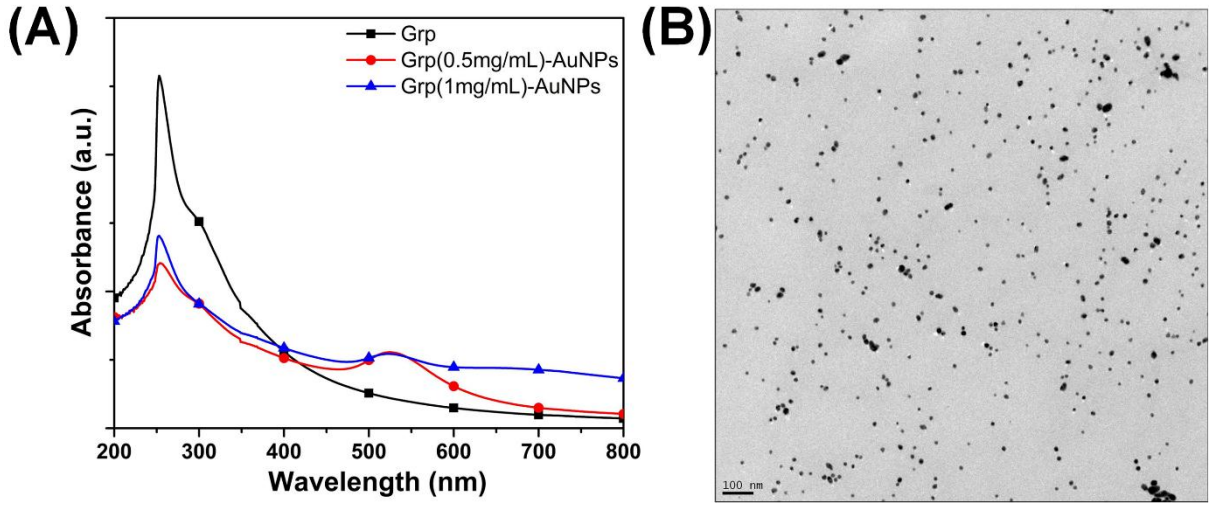

Fig. 2. Characterization of Grp-AuNPs composites: (A) UV-Visible spectroscopy of graphene and Grp-AuNPs composites, (B) TEM image of Grp-AuNPs (Grp=0.5 mg/mL) composite.

The modification of SPCE with Grp-AuNPs composites was validated by cyclic voltammetry (CV). The CV was performed in presence of 5 mM potassium ferricyanide/ferrocyanide redox couple prepared in 1X PBS. The CV of bare carbon (SPCE) and Grp-AuNPs composites is shown in Fig. S2. The redox probe $[Fe(CN)_6]^{3-/4-}$ revealed a reversible CV at the SPCE. After the deposition of nano-composites on SPCE, the current signal from $[Fe(CN)_6]^{3-/4-}$ greatly increased. The voltammetric data followed the similar trend with that of UV-visible spectroscopic and EDX analysis. A comparatively higher current was obtained from the SPCE with Grp-AuNPs (Grp=0.5 mg/mL) composite. It is believed that higher content of Grp resulted in masking of AuNPs surface and lower AuNPs to Grp ratio. Therefore, Grp-AuNPs composite with a Grp content of 0.5 mg/mL was used for further studies.

3.2 Optimization of norovirus aptasensor

The immobilization of the thiolated streptavidin on the Grp-AuNPs composite modified electrode was confirmed using CV in the presence of 5 mM $[Fe(CN)_6]^{3-/4-}$. After the Grp-AuNPs composite electrode was immobilized with thiolated streptavidin, the density and impedance of electrode increased, resulting in a decreased electrochemical signal (Fig. S2).

The immobilization and optimization of Bt-Apt-Fc concentration on streptavidin terminated electrode was confirmed by DPV studies in 1X PBS buffer. Aptamers with a varied concentration range of 0.25 µM to 1.5 µM were bonded with the streptavidin and the resulting current signal arising from tagged ferrocene was measured. Upon DPV study, the maximum current for the norovirus aptamer was obtained at a concentration of 1 µM, beyond which no further increase was observed (Fig. 3(A)). The immobilization presumably

saturated due to the exhaustion of free streptavidin on the electrode and steric hindrance between aptamers. These results confirmed that the immobilization of each intermediate layer had been successfully conducted. Therefore, 1 μM of aptamer was used for further aptasensing.

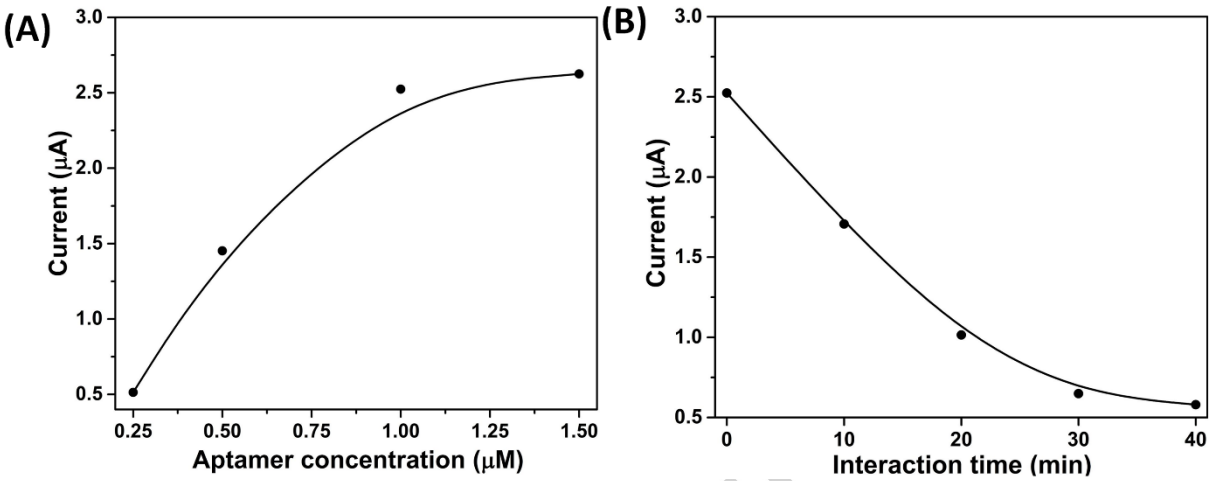

Fig. 3. Optimization of aptasensing: (A) Differential pulse voltammetric (DPV) signal of various concentration of ferrocene tagged aptamer on SPCE, (B) DPV signal after interaction of 3 nM norovirus with aptamer for different period. Buffer: 1X PBS.

The incubation time of aptamer and norovirus was optimized in order to obtain the maximum electrochemical signal and to perform the routine aptasensing within the shortest period of time. After the drop-casting 3 nM of norovirus on Bt-Apt-Fc terminated electrode, the mixtures were incubated for a period ranging from 10 to 40 min. The variation of the electrochemical signals during DPV in 1X PBS after interaction was recorded. As shown in Fig. 3(B), it was found that for the initial 10 min, the current decreased exponentially over time, reaching a minimum at 30 min. Therefore, to achieve high assay sensitivity, all of the following analyses were performed using 30 min interaction time.

3.3 Microfiltration in the microfluidic chip

The silica microbeads filter assists in faster sample processing without the need for a centrifuge or external filter. The filtration of clinical sample benefits in the removal of interfering agents and concentrate the analyte. The ability of microfilter to filter out a particulate suspension is shown in the Fig. 4. The inter-microbead space allows liquids and smaller sized molecules (Norovirus=25 – 35 nm) to pass through while hindering larger particulates. A bacterial culture broth was slowly injected in the microchannel and studied under an optical microscope to test the efficiency of microfiltration. Fig. 4(a and b) shows the inlet of microfilter at 4× and 20×, containing injected bacterial broth, respectively. After microfiltration, a visibly clean liquid free of debris and cell aggregates was released in the outlet (Fig. 4(c and d)). A simple syringe was used to inject the sample, instead of a syringe pump, which improves the portability of microfluidic aptasensor.

3.4 Microfluidic aptasensing of Norovirus

An all-PDMS and SPCE integrated microfluidic chip was fabricated to reduce the fabrication cost and time, along with increasing the disposability of the chip. The added advantages of integrating commercial SPCE include reliability and easy mass production capabilities. The detection mechanism for norovirus is described Fig. 1. The specific interaction of Bt-Apt-Fc immobilized on the electrode with norovirus results in an aptamer-norovirus complex. The capacitance of the electrode is increased due to the aptamer-norovirus complex and trapping of tagged ferrocene in the complex. An exponential decrease in the signal correlates to the concentration of norovirus present in the sample. The optimized aptasensing with 1 µM of aptamer on Grp-AuNPs composite and 30 min of interaction time was finally used for the detection of norovirus, as described in section 2.6.

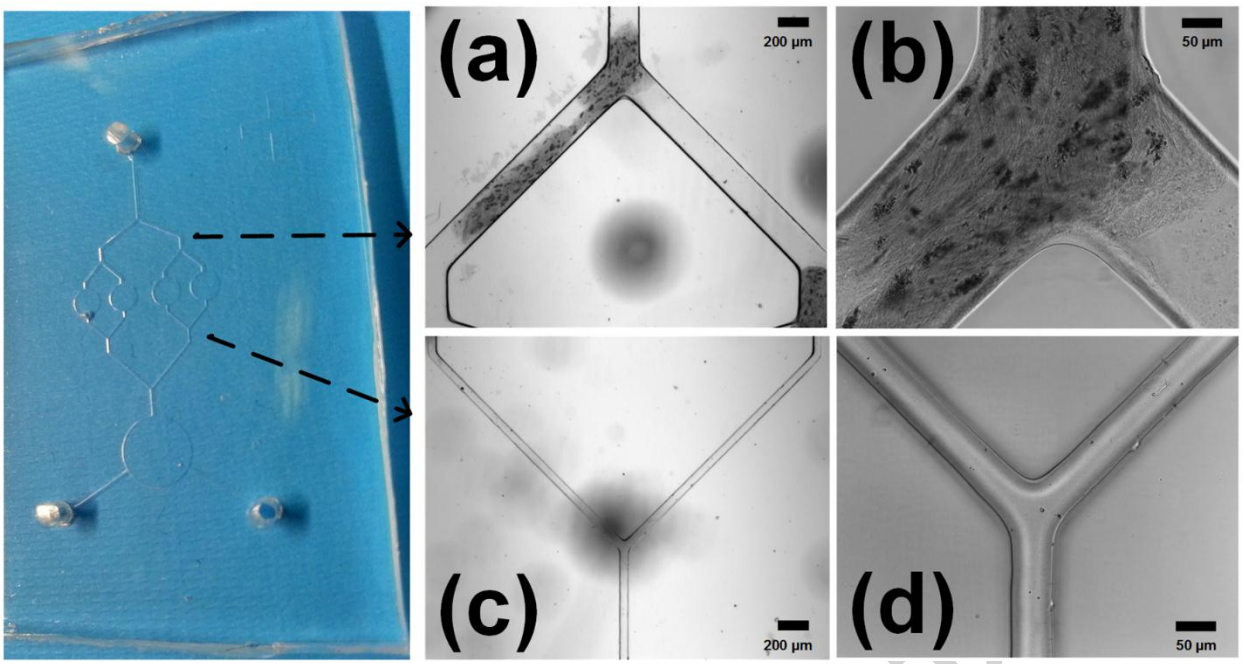

Fig. 4. Microfluidic sample processing: Microscopic image of bacterial culture in the microchannel at 4X and 20X before (a, b) and after (c, d) packed silica microbeads based filtration, respectively.

Fig. 5(A) represents the differential pulse voltammograms of microfluidic aptasensor studied with various concentrations (100 pM – 3.5 nM) of norovirus diluted in 1X PBS. It can be seen that the inherent cathodic peak current response from tagged ferrocene (E_{pa}=0.35 V) of the aptasensor in the absence of norovirus exhibited the highest peak current strength (2.52 µA). The consecutive study of different concentrations of norovirus reduced the peak current as the concentration increased. The 3.5 nM of norovirus produced the lowest peak current, signifying a high proportion of aptamer complex formation on the working electrode. Noticeable changes in the electrochemical signals were clearly observed as evident from the Fig. 5(A). A linear fit of the obtained current signal from DPV with respect to varying concentration of norovirus is plotted in Fig. 5(B). The values denote average current value (n=3) after baseline correction with standard deviation as error bars. A distinct change in the electrochemical signal was seen starting from 100 pM of norovirus. Linear fitting of the

results gave a correlation coefficient (R^2) of 0.989. From the electrochemical aptasensing of norovirus, the experimental detection limit was found to be 100 pM (n=3).

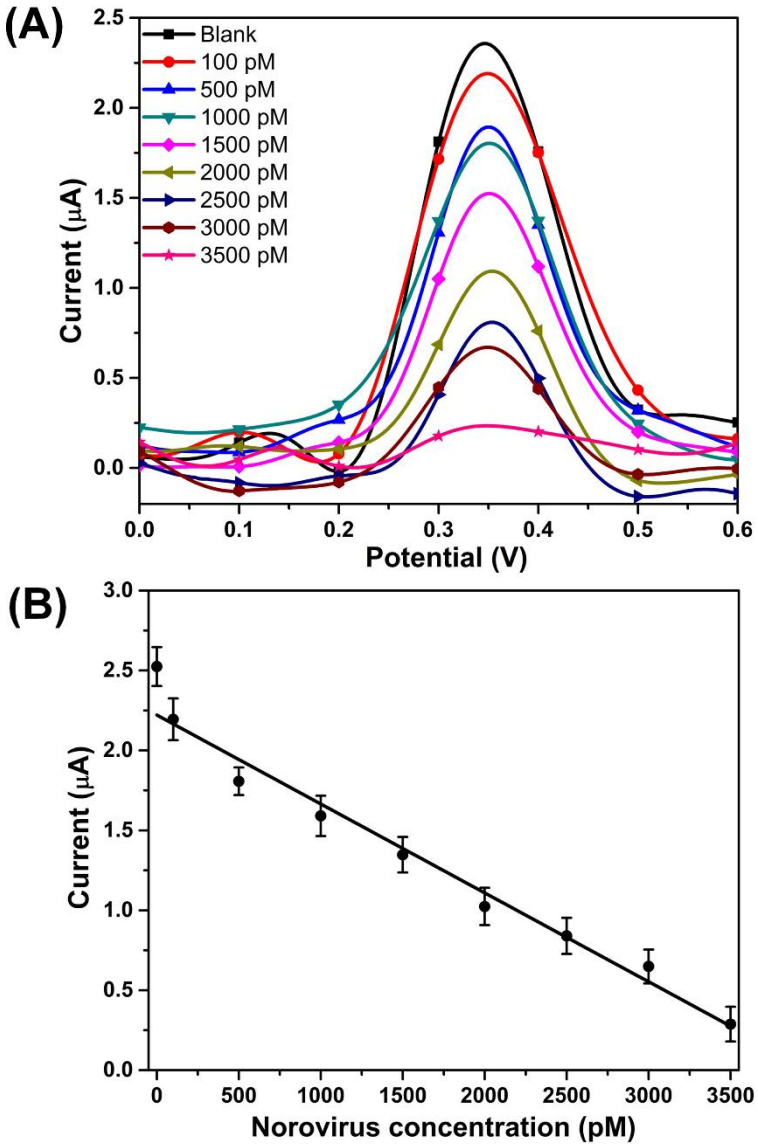

Fig. 5. Microfluidic electrochemical aptasensing of norovirus: (A) DPVs of various concentrations of norovirus on Grp-AuNPs composite and ferrocene tagged aptamer functionalized SPCE, (B) Calibration curve of norovirus aptasensing derived from the DPVs after baseline correction, R^2=0.989. Buffer: 1X PBS, Error bars: standard deviation (n=3).

Sometimes, the issue with designing an aptamer based biosensor is the high specificity of aptamer towards a particular genotype and variant only, which increases the risk of a false-negative signal. In the case of norovirus, although the GII.4 mediated infection is most

prevalent, GI, GII, and GIV as in whole are known to infect humans (White 2014). This work reports a point-of-care aptasensor for one-step sample purification and norovirus detection. As a proof-of-concept, commercially available GII/Beijing variant of norovirus was detected using an aptamer that is known to have good but varied sensitivity towards a broad range of norovirus genotypes (Escudero-Abarca et al., 2014). The sensitivities of previously reported norovirus biosensor are higher than the present work. However, carefully pairing the aptamer – norovirus system will help in increasing the sensitivity and utility of this biosensor. Quantitative microbial risk assessment studies (Lowther et al., 2012; Todd, 2016) on the risk of norovirus concentrations provides evidence that there is a substantial risk of illness when the concentrations exceed 2,000cpg. Hence, the sensitivity of this developed microfluidic biosensor is well above this threshold and holds good for real-time practical detection of noroviruses from clinical and complex sample matrices.

3.5 Aptasensing of norovirus in biological fluid

In order to verify the specificity of this detection methodology, at first, norovirus was detected in presence of peptidoglycan. The cell wall of most bacteria are made of peptidoglycan and is present in abundance in the fecal sample. To check the possible cross-reactivity between norovirus and bacterial 'shell' molecule, peptidoglycan solution (1 mg/mL) spiked with norovirus was analyzed in microfluidic aptasensor. As summarized in Table S1, the analysis of spiked norovirus exhibited an error margin of just 2-5%. This implies that the detection specificity of microfluidic aptasensor is not hampered by the presence of bacteria.

Table 1: Detection of norovirus concentration spiked in whole bovine blood.

Concentration spiked (pM)	Concentration detected (pM)	% Error
500	550.5	1.1
1000	1073.1	7.3
2000	2114.3	5.7
3000	3147.6	4.9

The practical application of proposed biosensor for detecting norovirus in the biological fluid was also validated. Different concentration of norovirus was spiked in the whole bovine blood and injected into the microchannel. The aptasensing was performed as described in the earlier sections. Table 1 summarizes the analysis of norovirus spiked in the blood. Marginally higher concentrations were sensed possibly due to the interference of unknown proteins present in the blood. However, the analysis showed good recoveries of the spiked norovirus. The average error margin was 5-10%. The total analysis time from injection to detection was around 35 min (aptamer-norovirus interaction time=30 min). These results clearly validate that the proposed microfluidic aptasensor can be successfully used for point-of-care one-step detection of norovirus in clinical samples.

4. Conclusions

This study reports a proof-of-concept microfluidic chip for the electrochemical detection of norovirus. An aptamer tagged with ferrocene, instead of $[Fe(CN)_6]^{3-/4-}$ as redox probe, was used for the selective detection of norovirus. The use of ferrocene as a redox probe enhanced the portability of biosensor. The Grp-AuNPs composite provided a stable substrate for aptamer immobilization and helped in signal amplification. Packed silica microbeads

facilitated an easy and rapid filtration of the biological fluid. DPV studies revealed a detection limit of 100 pM for recombinant norovirus-like particles. The aptasensor could also detect norovirus with high sensitivity and selectivity in the presence of peptidoglycan as an interferon. The total time of norovirus detection in the spiked blood sample was less than 35 min. The LOD of the aptasensor could be further enhanced by employing a specific aptamer. Rapid and on-site detection of norovirus during an outbreak is a major concern of health care professionals. The proposed microfluidic electrochemical aptasensor has the potential to be used as a point-of-care and one-step sample purification and norovirus detection.

Acknowledgments

The authors sincerely thank the Natural Sciences and Engineering Research Council of Canada (Grant# 400705) for funding this study.

References

Ahmed, S.R., Takemeura, K., Li, T.-C., Kitamoto, N., Tanaka, T., Suzuki, T., Park, E.Y., 2017. Biosens. Bioelectron. 87, 558-565.

Auer, S., Koho, T., Uusi-Kerttula, H., Vesikari, T., Blazevic, V., Hytönen, V.P., 2015. Sens. Actuators B Chem. 221, 507-514.

Beier, R., Pahlke, C., Quenzel, p., Henseleit, A., Boschke, E., Cuniberti, G., Labudde, D., 2014. FEMS Microbiol. Lett. 351, 162-169.

Bruin, E., Duizer, E., Vennema, H., Koopmans, M.P.G., 2006. J. Virol. Methods. 137, 259-264.

Chung, S.H., Baek, C., Cong, V.T., Min, J., 2015. Biosens. Bioelectron. 67, 625-633.

da Silva, E.T.S.G., Souto, D.E.P., Barragan, J.T.C., Giarola, J.F., de Moraes, A.C.M., Kubota, L.T., 2017. ChemElectroChem. 4, 778-794.

Dijksma, M., Boukamp, B.A., Kamp, B., van Bennekom, W.P., 2002. Langmuir. 18, 3105-3112.

Escudero-Abarca, B.I., Suh, S.H., Moore, M.D., Dwivedi, H.P., Jaykus, L.A., 2014. PLoS ONE. 9, e106805.

Fernandes, F.C.B., Santos, A., Martins, D.C., Góes, M.S., Bueno, P.R., 2014. Biosens. Bioelectron. 57, 96-102.

Friesema, I.H., Vennema, H., Heijne, J.C., de Jager, C.M., Morroy, G., van den Kerkhof, J.H., de Coster, E.J., Wolters, B.A., ter Waarbeek, H.L., Fanoy, E.B., Teunis, P.F., van der Linde, R., van Duynhoven, Y.T., 2009. Epidemiol. Infect. 137, 1722-1733.

Giamberardino, A., Labib, M., Hassan, E.M., Tetro, J.A., Springthorpe, S., Sattar, S.A., Berezovski, M.V., DeRosa, M.C., 2013. PLoS ONE. 8, e79087.

Hagström, A.E.V., Garvey, G., Paterson, A.S., Dhamane, S., Adhikari, M., Estes, M.K., Strych, U., Kourentzi, K., Atmar, R.L., Willson, R.C., 2015. PLoS ONE. 10, e0126571.

Halfon, P., Khiri, H., Gerolami, V., Bourliere, M., Feryn, J.M., Reynier, P., Gauthier, A., Cartouzou, G., 1996. J. Hepatol. 25, 307-311.

Hong, S.A., Kwon, J., Kim, D., Yang, S., 2015. Biosens. Bioelectron. 64, 338-344.

Hutson, A.M., Atmar, R.L., Estes, M.K., 2004. Trends Microbiol. 12, 279-287.

Hwang, H.J., Ryu, M.Y., Park, C.Y., Ahn, J., Park, H.G., Choi, C., Ha, S., Park, T.J., Park, J.P., 2017. Biosens.Bioelectron. 87, 164-170.

Jiang, X., Wang, M., Graham, D.Y., Estes, M.K., 1992. J. Virol. 66, 6527-6532.

Kageyama, T., Shigeyuki, K., Michiyo, S., Kazue, U., Shuetsu, F., Fuminori, B.H., Naokazu, T., Kazuhiko, K., 2003. J. Clin. Microbiol. 41, 1548-1557.

Kitajima, M., Wang, N., Tay, M.Q.X., Miao, J., Whittle, A.J., 2016. Micro. Nano. Lett. 11, 582-585.

Koo, H.L., Ajami, N., Atmar, R.L., DuPont, H.L., 2010. Discov. Med. 10, 61-70.

Lan, L., Yao, Y., Ping, J., Ying, Y., 2017. Biosens. Bioelectron. 91, 504-514.

Lowther, J. A., Gustar, N. E., Hartnell, R. E., Lees, D. N., 2012. J. Food. Protec. 75, 389-393.

Richards, G.P., Watson, M.A., Fankhauser, R.L., Monroe, S.S., 2004. Appl. Environ. Microbiol. 70, 7179-7184.

Scallan, E., Hoekstra, R.M., Angulo, F.J., Tauxe, R.V., Widdowson, M.A., Roy, S.L., Jones, J.L., Griffin, P.M., 2011. Emerg. Infect. Dis. 17, 7-15.

Shrivastava, S., Jadon, N., Jain, R., 2016. Trends Anal. Chem. 82, 55-67.

Song, K.-M., Lee, S., Ban, C., 2012. Sensors. 12, 612-631.

Teunis, P.F., Sukhrie, F.H., Vennema, H., Bogerman, J., Beersma, M.F., Koopmans, M.P., 2015. Epidemiol. Infect. 143, 1710-1717.

Todd, E. C. 2016. Foodborne Diseases: Case Studies of Outbreaks in the Agri-Food Industries. CRC Press. 318-240.

Veerapandian, M., Neethirajan, S., 2015. RSC Adv. 5, 75015-75024.

Vinje, J., Vennema, H., Maunula, L., Bonsdorff, C., Hoehne, M., Schreier, E., Richards, A., Green, J., Brown, D., Beard, S.S., Monroe, S.S., Bruin, E., Svensson, L., Koopmans, M.P.G., 2003. J. Clin. Microbiol. 41, 1423-1433.

Vogt, S., Su, Q., Gutierrez-Sánchez, C., Nöll, G., 2016. Anal. Chem. 88, 4383-4390.

White, P.A., 2014. Clin. Microbiol. Infec. 20, 741-745.

Wilhelmi de Cal, I., Revilla, A., Del Alamo, J.M., Román, E., Moreno, S., Sánchez-Fauquier, A., 2007. Clin. Microbiol. Infect. 13, 341-343.

Xiang, L., Wang, Z., Liu, Z., Weigum, S.E., Yu, Q., Chen, M.Y., 2016. IEEE Sens. J. 16, 8359-8364.

Yakes, B.J., Papafragkou, E., Conrad, S.M., Neill, J.D., Ridpath, J.F., Burkhardt III, W., Kulka, M., DeGrasse, S.L., 2013. Int. J. Food Microbiol. 162, 152-158.

Yoon, Y.-J., Li, K.H.H., Low, Y.Z., Yoon, J., Ng, S.H., 2014. Sens. Actuators B Chem. 198, 233-238.

Highlights

- A selective electrochemical aptasensor was fabricated for norovirus detection.
- Aptasensor was integrated with the all-PDMS microfluidic chip.
- Packed microbeads based filters were fabricated for rapid sample processing.
- Interaction of norovirus with redox-tagged aptamer resulted in a decrease of the signal.
- Rapid one-step detection of norovirus was conducted in spiked blood.